Progress In Electromagnetics Research C, Vol. 72, 29–41, 2017

A Miniaturized Volkswagen Logo UWB Antenna with Slotted Ground Structure and Metamaterial for GPS, WiMAX and WLAN Applications

Tanweer Ali* and Rajashekhar C. Biradar

Abstract—A novel concept of using slotted ground structure and a single circular split ring resonator (SRR) to achieve multiband operation from a miniaturized UWB antenna is presented in this paper. Initially, a miniaturized Volkswagen logo ultrawideband (UWB) antenna having −10 dB impedance bandwidth of about 124% (2.9–12.4 GHz) in simulation and 116.7% (3.1–11.8 GHz) under measurement is designed. This miniaturization leads to about 10% increment in −10 dB reflection coefficient bandwidth and about 66.71% reduction in the volume of the proposed UWB antenna as compared to the conventional circular antenna. In order to reconfigure the proposed UWB antenna to operate it at 1.5 (GPS), 3.5 (WiMAX), 5.2 and 5.8 GHz (WLAN) frequency bands, slotted ground structure with metamaterial is used. The proposed metamaterial is a circular SRR consisting of a single circular ring and is placed on the slotted ground structure of the proposed antenna to achieve 1.5 GHz band. The proposed configuration has a volume of $0.290\lambda_0 \times 0.290\lambda_0 \times 0.015\lambda_0$ ($30 \times 30 \times 1.6\,\text{mm}^3$) at a lower resonating band of 2.9 GHz and is fabricated on a widely available FR4 substrate with a loss tangent of 0.02 and dielectric constant of 4.4. Simulated and experimental results show that the proposed design yields $S_{11} < -10$ dB at the targeted frequencies. Good impedance matching, stable radiation characteristics with cross-polarization level less than −15 dB (both in E and H planes), VSWR < 2, average gain of 3.09 dBi and radiation efficiency of more than 85% are observed at the designed band when the antenna is fabricated and tested.

1. INTRODUCTION

The ultra wideband (UWB) technology has gained tremendous attention for its capabilities of short-range and wide bandwidth wireless communication. In contrast to the conventional narrowband communication systems, UWB systems transmit information efficiently and accurately by generating pulses at specific time intervals thus occupying a relatively large bandwidth. UWB technology has been a motivating factor in several potential applications due to its major characteristics such as a high bandwidth and data rate, thus providing secure communication in military applications. Additionally, the use of short pulses aids in reducing multipath channel fading capability since there is no overlap between the reflected and original signals. Given these aforementioned capabilities, numerous related topics pertaining to UWB systems have been proposed and studied for more than a decade [1–3].

Incorporating several communication standards within a single system is the major necessity of modern wireless communication. Several wideband, narrow band, dual band, ultra wideband, and multiband antennas are designed for achieving the aforementioned integration capability. Multiband antennas mitigate the effects of electromagnetic interference and pulse distortion thus offering preferred usage over ultra wideband antennas. Multiband antennas have the capability to integrate several

Received 1 December 2016, Accepted 9 January 2017, Scheduled 27 February 2017
* Corresponding author: Tanweer Ali (tanweers@reva.edu.in).
The authors are with the Wireless Communication Research Laboratory, School of Electronics & Communication Engineering, REVA University, Bangalore-560064, India.

communication standards into a single compact system in addition to low cost and high data rate features. Various multiband and UWB antennas with various structures have been reported in the literature [4]. Multiband antennas operate at multiple frequencies. Recently several techniques have been introduced for the design of multiband antennas. These include the use of multi-resonators [5], co-planar waveguides [6], defected microstrip structure [7], defected ground structure [8], coupling mechanism [9], reactive loads [10], fractalization [11], genetic optimization [12] and creation of slots [13–15].

There has been an ever-growing demand for antenna designs that provide effective integration capability. In order to meet this requirement, the antenna design must not only provide multiband operation but also possess a simple structure and compact size. In literature numerous low profile compact size dual band antennas limited to WLAN applications have been reported [16–20]. However, the design of an UWB antenna catering the requirements of multiple resonant modes is hardly reported. The use of miniaturized UWB antenna in conjunction with multiband operation leads to a notable progress in antenna performance as it leads to wider selection of frequencies and additionally mitigates the effects of electromagnetic interferences. The proposed design incorporates the major requisites for developing an optimum smart antenna technology.

The objective of this research work is to design a miniaturized Volkswagen logo UWB antenna with slotted ground structure and metamaterial for GPS, WLAN and WiMAX applications. The first step in the design constitutes the miniaturization of conventional circular UWB antenna using slotted ground structure. This miniaturization leads to about 10% increment in -10 dB reflection coefficient bandwidth and about 66.71% reduction in the volume of the proposed design as compared to conventional design.

In the second step, the above designed antenna is reconfigured for 1.5 (GPS), 3.5 (WiMAX), 5.2 and 5.8 GHz (WLAN) bands by using a single circular SRR (acting as metamaterial) and slotted ground structure. The proposed design shows -10 dB reflection coefficient of about 19.7% (1.46–1.78 GHz), 5.68% (3.42–3.62 GHz), 3.72% (5.1–5.29 GHz) and 6.95% (5.61–6.0 GHz) under simulation and 18.07% (1.56–1.87 GHz), 6.89% (3.36–3.60), 5.74% (4.9–5.19 GHz) and 5.04% (5.60–5.89 GHz) in measurement respectively.

For these designed bands, average radiation efficiency of 90.75% in simulation and 86.35% under measurement with a total measured gain of 3.09 dBi are observed. The negative permeability property of the proposed circular SRR is used to achieve 1.5 GHz (GPS) band. HFSS v.14.0 is used to simulate the designed antenna. In next sections we describe the miniaturization process, the multiband operation of the proposed antenna using slotted ground structure and metamaterial circular SRR. Also, the negative permeability retrieval mechanism is discussed in detail for the proposed single circular SRR. Conclusions are drawn at last.

2. MINIATURIZED VOLKSWAGEN LOGO UWB ANTENNA DESIGN

This section gives the design of proposed miniaturized UWB antenna. Miniaturization is obtained by cutting slots in the radiating patch and in the ground plane. The antenna design evolution of the proposed miniaturized Volkswagen logo UWB antenna is depicted in Figure 1. The introduction of slots disturbs the current distribution thereby increasing the effective inductance and line capacitance. In other words, there is an influence on the antenna current flow and impedance which correspondingly aids in the reduction of antenna size.

Initially, a circular patch UWB antenna is designed with a total dimension of $0.502\lambda_0 \times 0.502\lambda_0 \times 0.015\lambda_0$ (52 mm $\times$ 52 mm $\times$ 1.6 mm) using lumped port excitation. This antenna shows good radiation characteristics over a wide range of bandwidth. The rectangular slots in the ground plane of this antenna are used to achieve the UWB operation. The miniaturization of the existing antenna improves the overall performance particularly in terms of its applicability. The conventional antenna 'x' is miniaturized by cutting Volkswagen logo like slots in the radiating patch and rectangular slots in the ground plane. This miniaturization approach leads to about 10% increment in -10 dB reflection coefficient bandwidth and about 66.71% reduction in the volume of the proposed Volkswagen logo UWB antenna 'z' as compared to conventional circular UWB antenna 'x' illustrated in Figure 1(c). The total increase in impedance bandwidth and reduction in volume is mathematically calculated and represented in Table 1.

The simulation results of the configuration 'x', 'y' and 'z' are depicted in Figure 2. The simulation

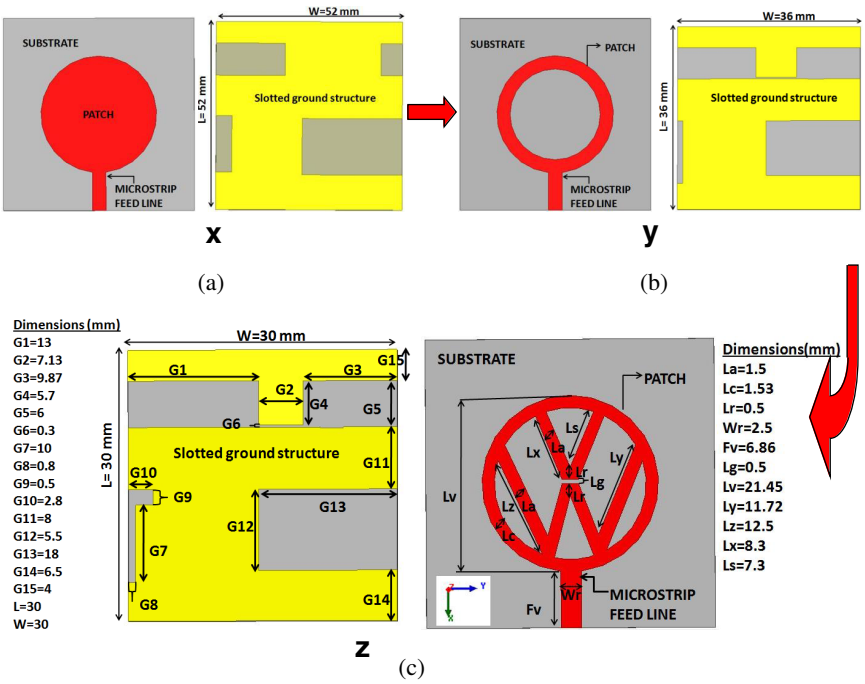

Figure 1. Evolution process of the proposed miniaturized UWB antenna with their front and ground structure (a) circular UWB antenna 'x'. (b) Miniaturized circular ring antenna 'y'. (c) Proposed miniaturized Volkswagen logo antenna 'z'.

Table 1. Comparison of antenna volume and -10 dB impedance bandwidth as per design evolution.

Parameter	Conventional circular shape UWB antenna	Circular ring UWB antenna	Proposed volkswagen logo antenna	Percentage Reduction (w.r.t conventional antenna)
Antenna volume (mm^3)	4326.4	2073.6	1440	66.71
Antenna -10 dB impedance bandwidth (%)	112	117	124	10

results show that all the three configurations have reflection coefficient (S_{11}) less than -10 dB.

The lowest resonant frequency of circular UWB antenna can be derived by Equation (1) [21].

$$f_r = \frac{1.8412 \cdot v_0}{2\pi \cdot a \cdot \sqrt{\varepsilon_{reff}}} \tag{1}$$

$$a = r\sqrt{\left\{1 + \frac{4H}{2\pi \cdot r \cdot \varepsilon_r}\left[\ln\left(\frac{2\pi \cdot r}{4H}\right) + 1.77\right]\right\}} \tag{2}$$

where v_0 is the velocity of light, and a and r are effective and physical radii of the circular patch antenna. The achieved -10 dB impedance bandwidths for configurations 'x', 'y' and 'z' are about 112% (3.4–12.4 GHz), 117% (3.7–12.6 GHz) and 124% (2.9–12.4 GHz), respectively. Thus the proposed miniaturized UWB antenna 'z' shows an improvement of 10% -10 dB reflection coefficient bandwidth compared to conventional circular UWB antenna 'x'.

In order to analyze the performance of the proposed design, parametric studies are carried out and shown in Figure 3.

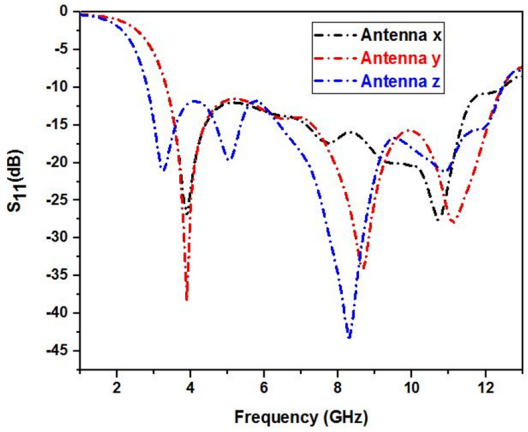

Figure 2. Simulation reflection coefficient (S_{11}) results for configuration 'x', 'y', 'z'.

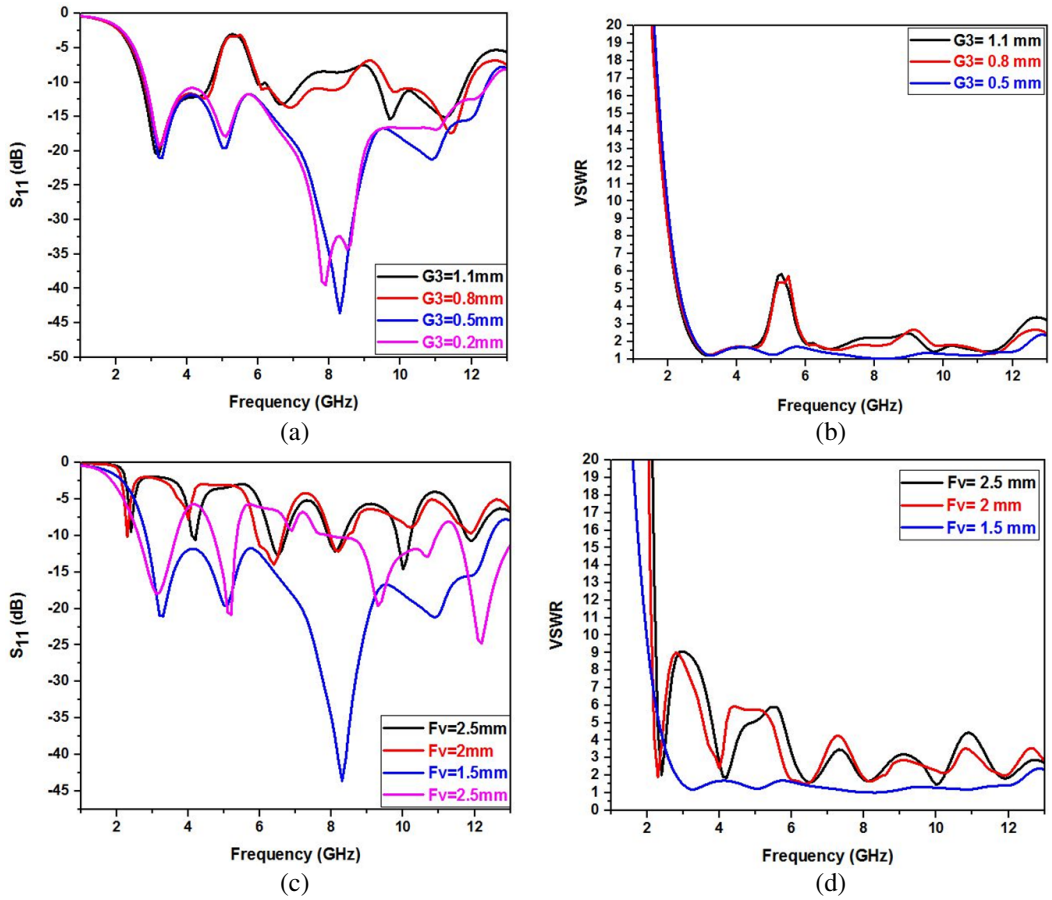

Figure 3. Parametric study of the proposed miniaturized UWB antenna. (a) and (b) S_{11} and VSWR variation for rectangular slot $G3$, (c) and (d) S_{11} and VSWR variation for feed length Fv.

First of all the effect of the slot ($G3 \times W$) is studied because this slot affects the performance of proposed design drastically compared to other slots. The effect is studied by keeping W constant and varying $G3$ dimension by 0.3 mm as shown in Figures 3(a), (b). From the graph, it is observed that with the increase in $G3$ dimension, reflection coefficient of the proposed design shifts above -10 dB and VSWR above 2. The best graph for the proposed UWB antenna is observed for $G3 = 0.5$ mm.

To meet the requirement of good impedance matching, the effect of feed line ($Fv \times Wr$) is studied and shown in Figures 3(c), (d). The study is done by keeping Wr (feed width) constant and varying Fv (feed length) by 0.5 mm. The study shows that with the increase in Fv, the proposed configuration loses its UWB characteristics. The resonance frequency and VSWR from 2.9 to 12.4 GHz are drastically affected. The best impedance matching is observed at $Fv = 1.5$ mm.

The simulated and experimental results of the proposed miniaturized Volkswagen logo UWB antenna are shown in Figure 4. The results show that the proposed design has a -10 dB reflection coefficient bandwidth of about 124% (2.9–12.4 GHz) under simulation and 116.7% (3.1–11.8 GHz) in measurement.

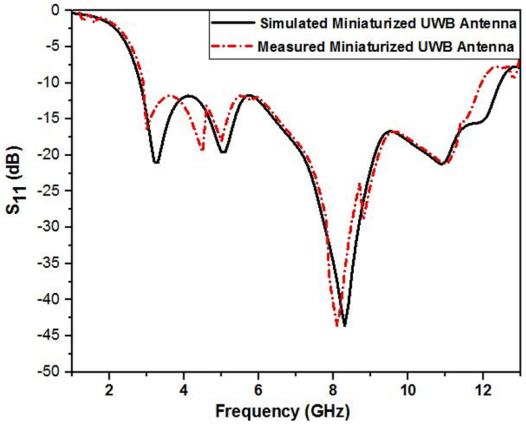

Figure 4. Simulated and measured S_{11} of the proposed miniaturized Volkswagen logo antenna.

3. TRIPLE BAND ANTENNA DESIGN

The miniaturization of the proposed Volkswagen logo UWB antenna is successfully carried out in Section 2. The miniaturized UWB antenna exhibits good impedance matching, -10 dB impedance bandwidth and VSWR for the frequency band ranging from 2.9 to 12.4 GHz. In order to achieve other useful wireless frequency bands, this miniaturized UWB antenna can be reconfigured by cutting additional rectangular slots in the ground plane apart from the existing ones. The process of modifying the ground structure of the miniaturized UWB antenna in order to obtain triple band is shown in Figure 5. As per the design evolution of Figure 5, the rectangular slots ($G17 \times G26$), ($G13 \times G12$), ($G6 \times G11$), ($G10 \times G9$) and ($G18 \times G2$) are introduced in the ground plane of the proposed UWB antenna without modifying the front Volkswagen logo radiating patch. The introduction of these slots creates additional current path length which disturbs the surface current distribution of UWB antenna thereby making it resonate at 3.2 (WiMAX), 5.1 and 5.7 GHz (WLAN) bands. The detailed optimized dimensions of the triple band antenna are further given in the proposed antenna design as shown in Figure 8.

The evolution stage simulation results of the three antennas are illustrated in Figure 6. From the simulation result, it is observed that Antenna 1 operates at single band (3.9 GHz); Antenna 2 operates at dual bands (5 and 7.2 GHz); Antenna 3 operates at triple bands (3.2, 5.1 and 5.7 GHz). Figure 6 shows that Antenna 3 yields -10 dB impedance bandwidth of about 6.85% (3.1–3.32 GHz), 3.92% (5.0–5.2 GHz) and 3.5% (5.7–5.9 GHz) at 3.1, 5.1 and 5.8 GHz, respectively.

In order to analyze the effect of introduced slots on Antenna 3 performances, parametric analysis is done and shown in Figure 7. This study is carried out first on rectangular slot ($G13 \times G12$). The study is done by keeping $G12$ constant and varying $G13$ by 0.5 mm as illustrated in Figure 7(a). The study shows that with the variation in $G13$, reflection coefficient decreases, and there is a shift in resonance frequency. The best result is obtained for $G13 = 4$ mm.

To analyze the effect of rectangular slot ($G17 \times G18$) on Antenna 3 impedance matching its analysis is also done. The study is done by keeping constant $G18$ and varying $G17$ by 0.5 mm as shown in

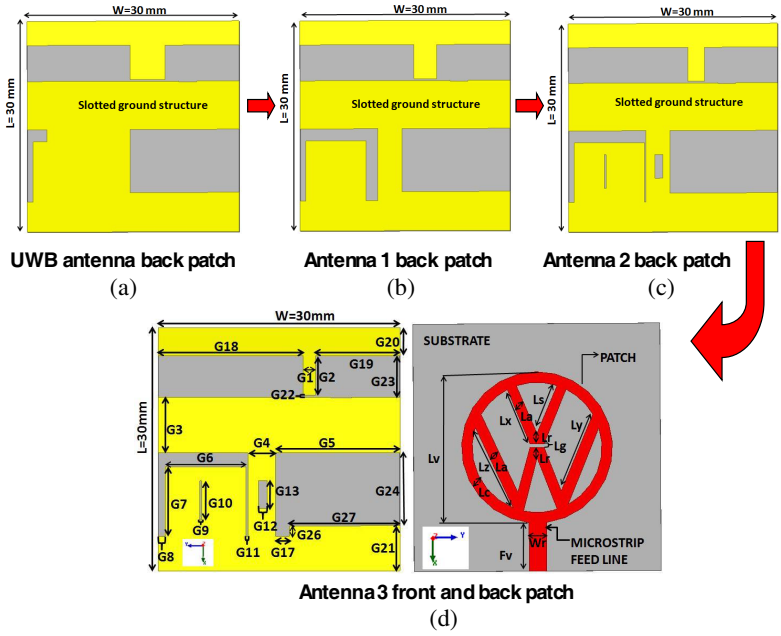

Figure 5. Evolution layout of the triple band antenna showing a modification in the ground structure using rectangular slots to obtain triple band resonance from proposed UWB antenna. (a) Proposed miniaturized UWB antenna back patch (b), (c) and (d) Antenna 1, 2, and 3 modified ground plane.

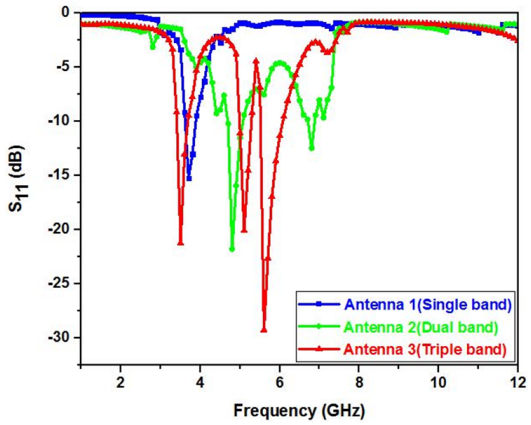

Figure 6. Simulation S_{11} result of Antenna 1, 2 and 3 showing single, double and triple band respectively.

Figure 7(b). From the study, it is clear that resonance as well as reflection coefficient is disturbed as $G17$ is varied. The best impedance matching is observed for $G17 = 2\,\text{mm}$.

4. PROPOSED ANTENNA DESIGN

Initially, a Volkswagen logo UWB antenna is designed and then subsequently redesigned by creating additional slots in the ground plane to achieve triple band of resonance as shown in Figure 6 (Antenna 3). These slots disturb the surface current density of proposed UWB antenna thereby creating additional current path length, thus making the redesigned antenna to operate at triple resonance. In order to operate this antenna for one more band, i.e., 1.5 GHz (GPS band), a single circular SRR (acting as metamaterial) is loaded partially in the ground plane of the triple band antenna. The proposed miniaturized Volkswagen logo UWB antenna with slotted ground structure and a single circular SRR

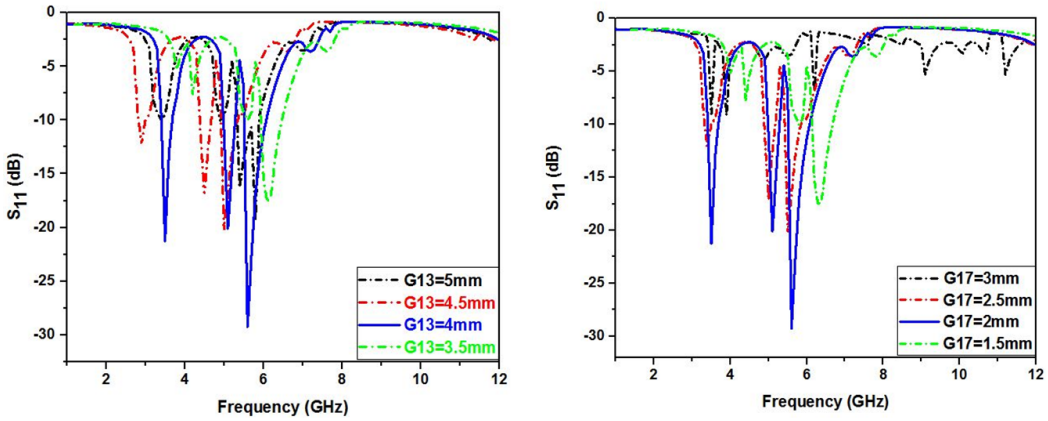

Figure 7. Parametric study of Antenna 3. (a) Effect of slot $G13$ on Antenna 3 performance. (b) Impedance matching variation of Antenna 3 with the variation in $G17$.

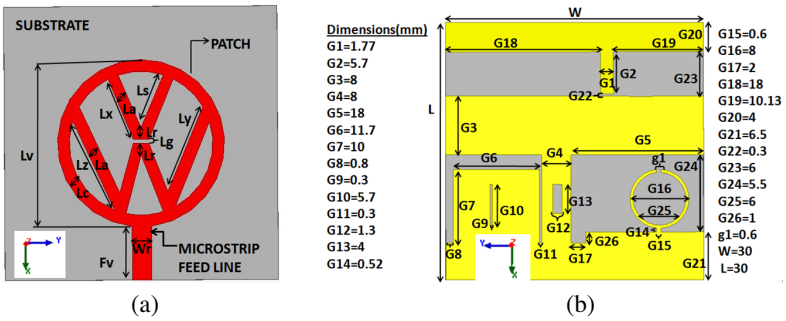

Figure 8. Proposed Volkswagen logo antenna with slotted ground structure and metamaterial circular SRR for 1.5 (GPS), 3.5 (WiMAX), 5.2 and 5.8 GHz (WLAN) frequency bands. (a) Front view. (b) Back view [Note — The front view dimensions are same as illustrated in Figure 1(c).]

is depicted in Figure 8. The introduction of this SRR creates a solenoidal current with time fluctuating magnetic field which generates a magnetic response from the conductor thereby exhibiting a resonance at 1.5 GHz. The resonance frequency of the circular SRR can be calculated by Equation (3) [22].

$$f_r = \frac{c}{2\pi^2}\sqrt{\frac{3(r_2 - r_1 - w)}{Re(\varepsilon_r)r_1^3}} \tag{3}$$

The measurement of the complex permeability and permittivity of materials over wide range of microwave frequencies from their time-domain transient response was proposed by Nicholson-Ross-Weir (NRW) [23]. Smith et al. utilized the material parameter extraction technique based on the NRW reflection and transmission measurements [24]. Figure 9(a) demonstrates the setup used for waveguide in HFSS that is correspondingly required for the calculation S_{21} and S_{11} for the proposed circular SRR. The empirical investigation requires the resonator to be placed within the waveguide medium as stated in [24]. An EM signal is incident via one port, and the values of S_{11} and S_{21} can be obtained by extracting the viable medium parameters. The magnetic permeability (μ) is retrieved by the S_{11} and S_{21} obtained from the HFSS simulated waveguide environment. Mathematically, μ is calculated as a product of impedance (z) and refractive index (n) ($\mu = z \times n$). The values of n and z are calculated as [24–26] given in Equations (4) and (5), respectively.

$$n = \frac{1}{kd}\cos^{-1}\left[\frac{1}{2s_{21}}\left(1 - s_{11}^2 + s_{21}^2\right)\right] \tag{4}$$

$$z = \sqrt{\frac{(1+s_{11})^2 - s_{21}^2}{(1-s_{11})^2 - s_{21}^2}} \tag{5}$$

The simulation based S-parameters representing stopband phenomenon of the split ring resonator at a frequency of 1.5 GHz is illustrated in Figure 9(b). The reflection (S_{11}) and transmission coefficient (S_{21}) at this frequency are less than -2 dB and -10 dB, respectively. The retrieved negative permeability of circular SRR at this frequency (1.5 GHz) is illustrated in Figure 9(c).

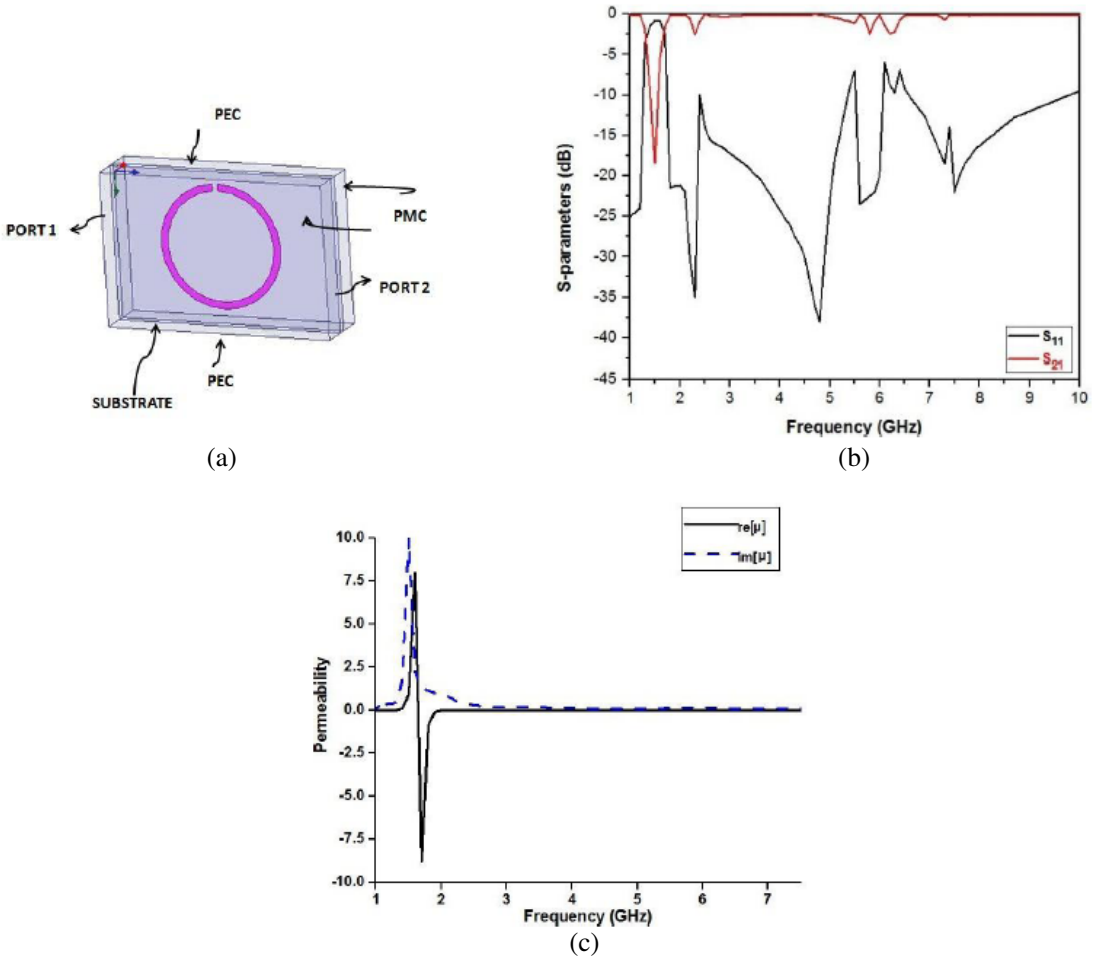

Figure 9. Extraction of negative permeability of the proposed circular SRR (a) waveguide set up for extracting of S-parameters. (b) Stop band phenomenon of circular SRR exhibiting S_{11} almost near to zero and S_{21} less than -10 dB. (c) Retrieved negative permeability at 1.5 GHz band.

The proposed design is initially simulated on HFSS v.14.0 software and then fabricated on a low cost widely available FR4 substrate with loss tangent = 0.03, thickness $h = 1.6$ mm and dielectric constant $\varepsilon_r = 4.4$. The prototype of the proposed design and its simulation and experimental results are illustrated in Figure 10.

From Figure 10(b), it is observed that the reconfigured proposed UWB antenna now operates at 1.5 GHz, 3.5 GHz, 5.2 GHz and 5.8 GHz, respectively. There is a shift observed at the resonating band 3.5 GHz compared to the result of triple band antenna which may be due to the introduction of circular SRR in the ground plane. Thus, the proposed design is successfully achieved by using metamaterial circular SRR and slotted ground structure. The results show that the proposed configuration yields -10 dB impedance bandwidth of about 19.7% (1.46–1.78 GHz), 5.68% (3.42–3.62 GHz), 3.72% (5.1–5.29 GHz) and 6.95% (5.61–6.0 GHz) under simulation and 18.07% (1.56–1.87 GHz), 6.89% (3.36–3.60),

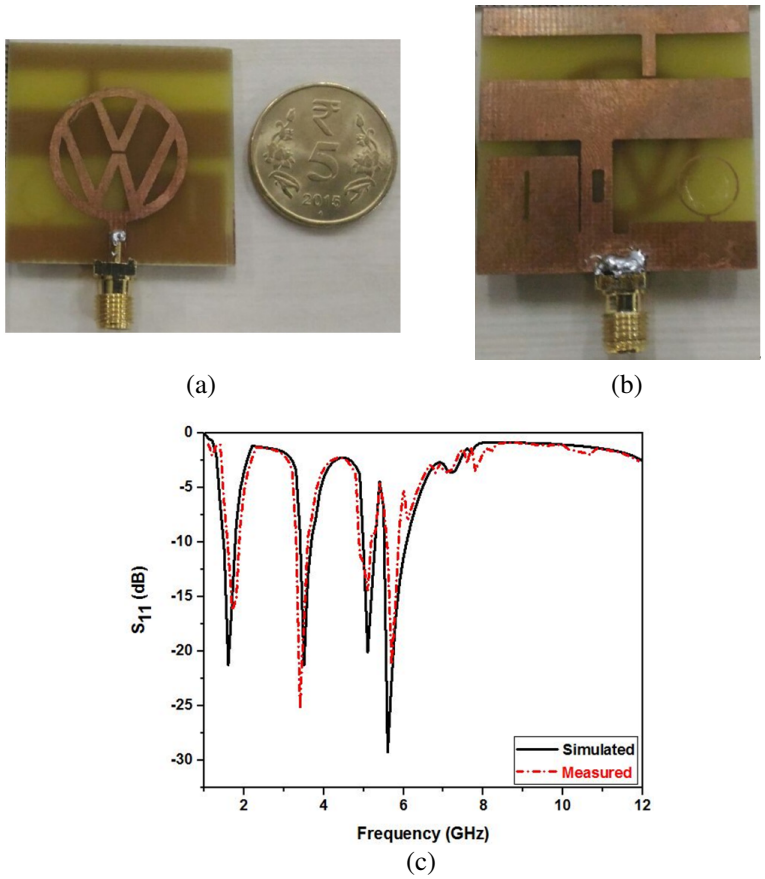

Figure 10. Fabricated model and experimental result of the proposed design. (a) Fabricated antenna front and back view. (b) Simulated and measured S_{11} results.

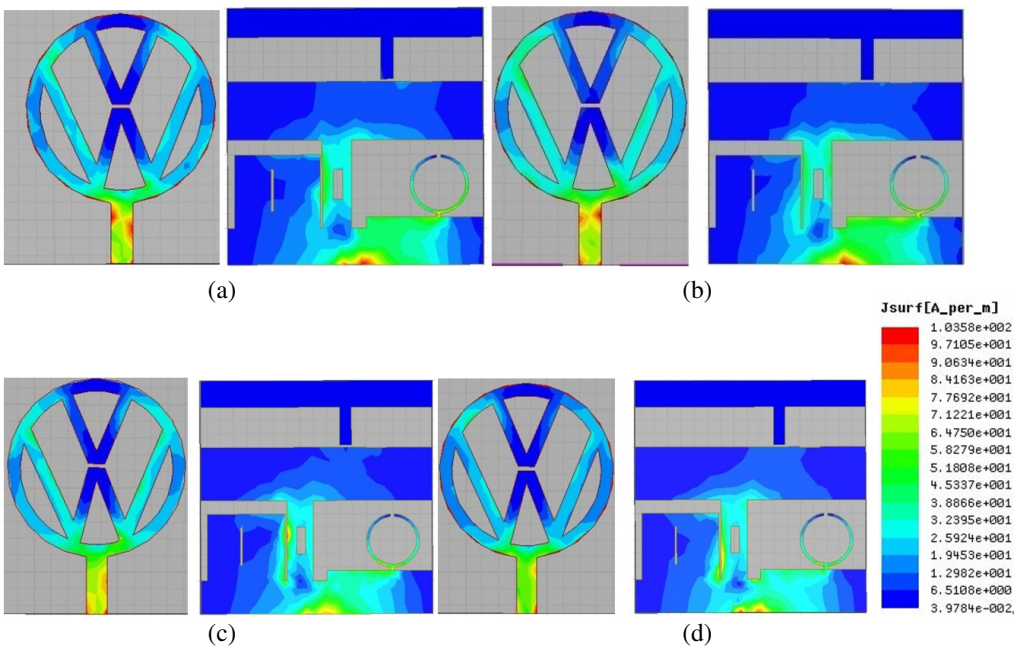

Figure 11. Surface current distribution of the proposed configuration at (a) 1.5 GHz, (b) 3.5 GHz, (c) 5.2 GHz and (d) 5.8 GHz.

5.74% (4.9–5.19 GHz) and 5.04% (5.60–5.89 GHz) in measurement respectively. The slotted ground structure and circular SRR dimensions are optimized to obtain the desired results. Experimental results are slightly deviated from the simulated ones, which may be due to fabrication process and SMA connectors soldering. However, the achieved bandwidth is sufficient to meet the requirement of GPS, WiMAX and WLAN applications. The resonant mode operation of the proposed antenna at

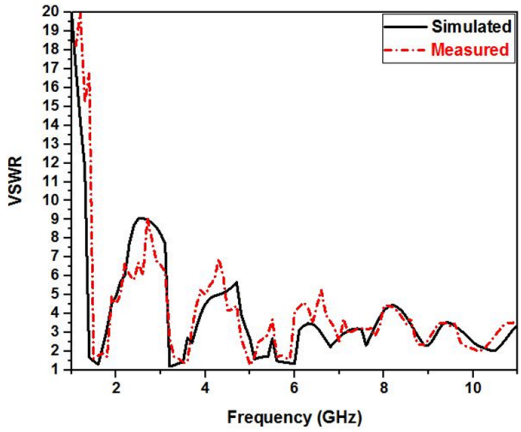

Figure 12. Simulated and measured VSWR for the proposed design.

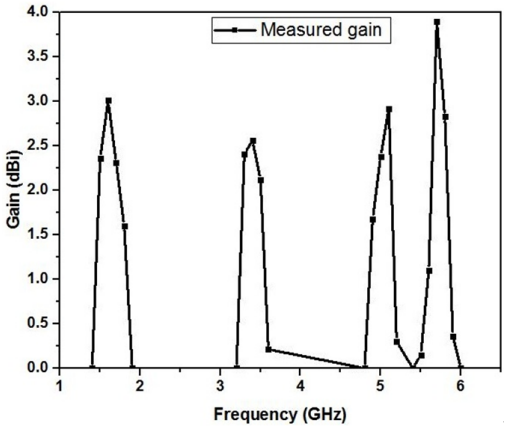

Figure 13. Measured gain at 1.6, 3.46, 5.18 and 5.76 GHz.

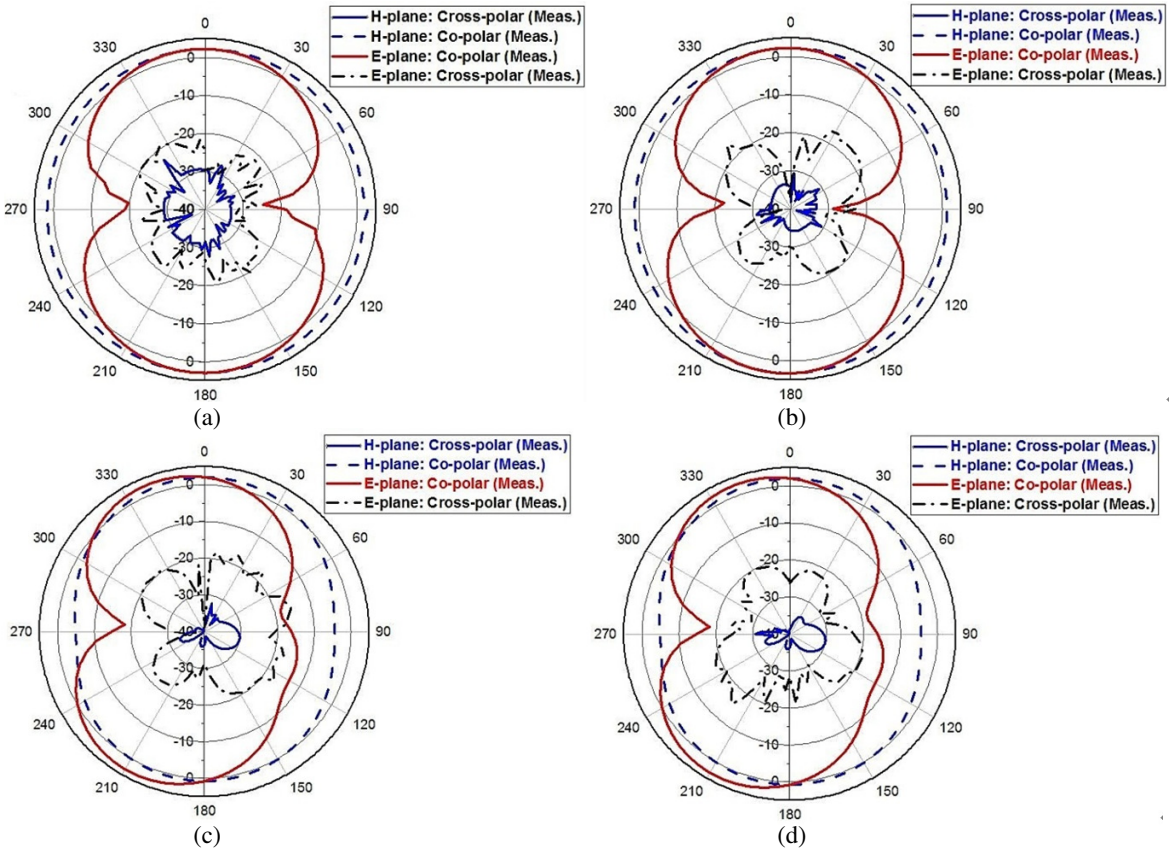

Figure 14. Measured radiation characteristics of the proposed design at (a) 1.6, (b) 3.46, (c) 5.18, (d) 5.76 GHz.

1.5, 3.5, 5.2 and 4.8 GHz can easily be analyzed by observing the surface current distribution plot as illustrated in Figure 11.

Practically for proper operation of antenna VSWR should be between 1 and 2. From Figure 12 it is observed that the proposed design has VSWR < 2 in both simulation and measurement for the design frequency band. The measured VSWR shows some glitches which may be due to fabrication and measurement tolerance.

The antenna gain is computed by gain transfer method by keeping horn antenna as a reference antenna in anechoic chamber. The measured gain of the proposed design is illustrated in Figure 13. The measured peak gains of 3.01, 2.56, 2.92 and 3.9 dBi are observed for 1.6, 3.46, 5.18 and 5.76 GHz, respectively.

The measured H-plane and E-plane radiation characteristics for the proposed configuration at 1.6, 3.46, 5.18 and 5.76 GHz are depicted in Figure 14. Both in E and H-planes the measured cross polarization levels are less than -15 dB. The radiation pattern of the proposed design resembles bidirectional radiation pattern in E-plane and omnidirectional radiation characteristics in H-plane. The omnidirectional radiation pattern favors the usage of proposed antenna in remote application for the desired bands.

The simulated and measured radiation efficiencies of the proposed configuration are shown in Figure 15. It is observed that the measured radiation efficiency remains more than 85% for all the four designed bands. The proposed antenna exhibits measured radiation efficiencies of 91%, 85.5%, 87% and 86% at 1.6 (GPS), 3.46 (WiMAX), 5.18 and 5.76 GHz (WLAN) bands, respectively.

The proposed configuration performance in terms of size, number of operating bands and gain is compared with other important existing antennas in the literature as depicted in Table 2. This comparison shows that the proposed configuration has better performance characteristics in terms of the parameters compared.

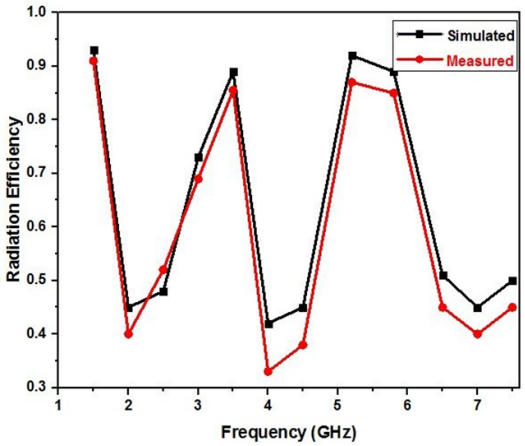

Figure 15. Simulated and experimented radiation efficiencies for the proposed configuration.

Table 2. Comparison of present work with existing in the literature.

Ref.	Size (mm^3)	No. of operating bands	Gain (dBi) at operating bands	Bandwidth (%) at operating bands
[27], 2013	$32 \times 14 \times 0.8$	3 (2.6/3.5/5 GHz)	1.3/2.4/3.5	16.6/2.4/3.5
[28], 2010	$35 \times 30 \times 1.6$	3 (2.5/3.5/5.5 GHz)	1.3/2.3/3.4	22.2/12.3/23.2
[29], 2011	$28 \times 32 \times 1.6$	3 (2.5/3.5/5.15 GHz)	1.3/2.3/3.2	18.6/24.9/13.5
[30], 2008	$34 \times 15 \times 1.6$	3 (2.4/3.5/5 GHz)	3.9/1.95/2.82	13.4/14.4/26
[31], 2015	$48 \times 18 \times 1.6$	4 (1.3/2.3/3.5/5.2 GHz)	1.3/2.3/3.5/4.4	7.2/6.33/18.2/4.6
Proposed	$\mathbf{30 \times 30 \times 1.6}$	**4 (1.5/3.5/5.2/5.8 GHz)**	**3.01/2.56/2.92/3.9**	**19.7/6.89/5.7/5.04**

5. CONCLUSION

The proposed Volkswagen logo antenna with slotted ground structure and circular SRR fed by 50 Ω microstrip feed line using lumped port excitation is successfully designed, simulated and implemented in order to validate the empirical designs. The targeted frequencies 1.5, 3.5, 5.2 and 5.8 GHz of the proposed antenna easily meet the GPS, WiMAX and WLAN requirements. Parametric studies are done to analyze the performance of the proposed design. This analysis shows that slight change in rectangular slots dimensions perturbs the surface current distribution thereby drastically affecting the impedance matching and resonance characteristics of the proposed configuration. The designed antenna shows good measured radiation characteristics with cross polarization level less than −15 dB in both E and H planes. The omnidirectional pattern in H-plane favors the usage of the proposed antenna in remote location for the designed bands. Moreover, the proposed design is compact and can be easily integrated with wireless terminal devices. Good gain, stable radiation characteristics and good radiation efficiency make the proposed design suitable for GPS, WiMAX and WLAN applications. Future work involves the reconfiguration of the designed band from one frequency to another or simultaneously to two frequencies using PIN or varactor diode switch.

REFERENCES

1. Tang, M. C., H. Wang, T. Deng, and R. W. Ziolkowski, "Compact planar ultra-wideband antennas with continuously tunable independent band-notched filters," *IEEE Trans. on Antennas and Propag.*, Vol. 64, No. 8, 3292–3301, 2016.
2. Tang, M. C., T. Shi, and R. W. Ziolkowski, "Planar ultrawideband antennas with improved realized gain performance," *IEEE Trans. on Antennas and Propag.*, Vol. 64, No. 1, 61–69, 2016.
3. Kumar, M., A. Basu, and S. K. Koul, "UWB printed slot antenna with improved performance in time and frequency domains," *Progress In Electromagnetics Research C*, Vol. 18, 197–210, 2011.
4. Dang, L., Z. Y. Lei, Y. J. Xie, G. L. Ning, and J. Fan, "A compact microstrip slot triple-band antenna for WLAN/WiMAX applications," *IEEE Antennas and Wirel. Propag. Lett.*, Vol. 9, 1178–1181, 2010.
5. Baek, S. and Y. Jee, "Compact integrated monopole antenna with CPW-fed meander resonators," *Electron. Lett.*, Vol. 47, No. 2, 79–80, 2011.
6. Liu, P., Y. Zou, B. Xie, X. Liu, and B. Sun, "Compact CPW-fed tri-band printed antenna with meandering split-ring slot for WLAN/WiMAX applications," *IEEE Antennas and Wirel. Propag. Lett.*, Vol. 11, 1242–1244, 2012.
7. Peyrot-Solis, M. A., J. A. Tirado-Mendez, and H. Jardon-Aguilar, "Design of multiband UWB planarized monopole using DMS technique," *IEEE Antennas and Wirel. Propag. Lett.*, Vol. 6, 77–79, 2007.
8. Zulkifli, F. Y., E. T. Rahardjo, and D. Hartanto, "Mutual coupling reduction using dumbbell defected ground structure for multiband microstrip antenna array," *Progress In Electromagnetics Research Letters*, Vol. 13, 29–40, 2010.
9. Risco, S., J. Anguera, A. Andujar, A. Perez, and C. Puente, "Coupled monopole antenna design for multiband handset devices," *Microw. Opt. Technol. Lett.*, Vol. 52, No. 2, 359–364, 2008.
10. Richards, W. F., S. E. Davidson, and S. A. Long, "Dual band, Reactively loaded microstrip antenna," *IEEE Trans. on Antennas and Propag.*, Vol. 33, 556–561, 1985.
11. Puente, C., J. Anguera, C. Borja, and J. Soler, "Fractal-Shaped antennas and their application to GSM 900/1800," Vol. 2, 2001.
12. Jayasinghe, J. W., J. Anguera, and D. N. Uduwawala, "A simple design of multi band microstrip patch antennas robust to fabrication tolerances for GSM, UMTS, LTE, and Bluetooth applications by using genetic algorithm optimization," *Progress In Electromagnetics Research M*, Vol. 27, 255–269, 2012.

13. Hongnara, T., C. Mahattanajatuphat, P. Akkaraekthalin, and M. Krairiksh, "A multiband CPW-fed slot antenna with fractal stub and parasitic line," *Radioengineering*, Vol. 21, No. 2, 597–605, 2012.
14. Zhang, S. M., F. S. Zhang, W. M. Li, W. Z. Li, and H. Y. Wu, "A multi-band monopole antenna with two different slots for WLAN and WiMAX applications," *Progress In Electromagnetics Research Letters*, Vol. 28, 173–181, 2012.
15. Elsheakh, D. M. and E. A. Abdallah, "Compact multiband multifolded-slot antenna loaded with printed-IFA," *IEEE Antennas and Wirel. Propag. Lett.*, Vol. 11, 1478–1481, 2012.
16. Su, S. W., "Compact four loop antenna system for concurrent, 2.4 and 5 GHz WLAN operation," *Microw. Opt. Techon. Lett.*, Vol. 56, No. 1, 208–215, 2014.
17. Huang, C.-Y. and E.-Z. Yu, "A slot-monopole antenna for dual-band WLAN applications," *IEEE Antennas and Wirel. Propag. Lett.*, Vol. 10, 500–502, 2011.
18. Chien, H. Y. and C. H. Lee, "Dual-band meander monopole antenna for WLAN operation in laptop computer," *IEEE Antennas and Wirel. Propag. Lett.*, Vol. 12, 694–697, 2013.
19. Ghatak, R., R. K. Mishra, and D. R. Poddar, "Perturbed Sierpinski carpet antenna with CPW feed for IEEE 802.11 a/b WLAN application," *IEEE Antennas and Wirel. Propag. Lett.*, Vol. 7, 742–744, 2008.
20. Rao, Q. and W. Geyi, "Compact multiband antenna for handheld devices," *IEEE Trans. on Antennas and Propag.*, Vol. 57, No. 10, 3337–3339, 2009.
21. Balanis, C. A., *Antenna Theory Analysis and Design*, Wiley Publication, 2005.
22. Pandeeswari, R. and S. Raghavan, "A CPW fed triple band OCSRR embedded monopole antenna with modified ground for WLAN and WIMAX applications," *Microw. and Opt. Techn. Lett.*, Vol. 57, No. 10, 2413–2418, 2015.
23. Nicolson, A. M. and G. F. Ross, "Measurement of the intrinsic properties of materials by time-domain techniques," *IEEE Trans. on Instr. and Meas.*, Vol.19, No. 4, 377–382, 1970.
24. Smith D. R., S. Schultz, P. Markos, and C. M. Soukoulis, "Determination of negative permittivity and permeability of metamaterials from reflection and transmission coefficients," *Phys. Rev. B*, Vol. 65, 195104–9, 2002.
25. Chen, H., J. Zhang, Y. Bai, Y. Luo, L. Ran, and Q. Jiang, "Experimental retrieval of the effective parameters of metamaterials based on a waveguide method," *Opt. Express*, Vol. 14, No. 26, 12944–12949, 2006.
26. Smith, D. R., D. C. Vier, T. Koschny, and C. M. Soukoulis, "Electromagnetic parameter retrieval from in homogeneous metamaterials," *Phys. Rev. B*, Vol. 71, 36617–27, 2005.
27. Lu, J. H. and B. J. Huang, "Planar compact slot antenna with multiband operation for IEEE 802.16 m application," *IEEE Trans. on Antennas and Propag.*, Vol. 61, No. 3, 1411–1414, 2013.
28. Dang, L., Z. Y. Lei, Y. J. Xie, G. L. Ning, and J. Fan, "A compact microstrip slot triple-band antenna for WLAN/WiMAX applications," *IEEE Antennas Wireless Propag. Lett.*, Vol. 9, 1178–1181, 2010.
29. Hu, W., Y. Z. Yin, P. Fei, and X. Yang, "Compact triband square-slot antenna with symmetrical L-Strips for WLAN/WiMAX applications," *IEEE Antennas Wireless Propag. Lett.*, Vol. 10, 462–465, 2011.
30. Lee, Y.-C. and J.-S. Sun, "Compact printed slot antennas for wireless dual and multiband operation," *Progress In Electromagnetics Research*, Vol. 88, 289–305, 2008.
31. Cao, Y. F., S. W. Cheung, and T. I. Yuk, "A multiband slot antenna for GPS/WiMAX/WLAN applications," *IEEE Trans. on Antennas and Propag.*, Vol. 63, No. 3, 952–958, 2015.